Journal of Molecular Liquids 358 (2022) 119081

Contents lists available at ScienceDirect

Journal of Molecular Liquids

journal homepage: www.elsevier.com/locate/molliq

Conformational binding mechanism of lysozyme induced by interactions with penicillin antibiotic drugs

Ramón Rial [a], Michael González-Durruthy [a], Zhen Liu [b], Juan M. Ruso [a,*]

[a] Soft Matter and Molecular Biophysics Group, Department of Applied Physics, University of Santiago de Compostela, 15782 Santiago de Compostela, Spain
[b] Department of Physics and Engineering, Frostburg State University, Frostburg, Maryland 21532, United States

ARTICLE INFO

Article history:
Received 21 December 2021
Revised 22 March 2022
Accepted 31 March 2022
Available online 21 April 2022

Keywords:
Lysozyme
Antibiotic
Molecular docking
Protein interactions

ABSTRACT

In this study we present an in-depth and detailed analysis of the binding process between two antibiotics (cloxacillin and dicloxacillin) and a blood serum protein (lysozyme). Our objectives have been several: to determine, at the atomic level, the structural and conformational changes that take place in both molecular structures once the complex is formed; to investigate the effect that the substitution of a hydrogen atom for a chlorine atom has on the bonding process; and to relate these local modifications with macromolecular parameters. Achieving these goals requires a multi-pronged approach and effective resource management. In our case, we have combined different experimental (isothermal titration calorimetry, UV–vis and fluorescence spectroscopy) and computational techniques (molecular docking and network models), in order to obtain comprehensive and contrasted information of the interaction process. Both approaches have showed an excellent correlation, confirming that there is a single binding site, that both penicillins are moderate binders and hydrogen bond and van der Waals forces are predominant. On the other hand, the small discrepancies between the two techniques highlighted the pressing need to approach the study of these systems from both atomic and macromolecular perspectives.

1. Introduction

Studying the molecular interactions involved in protein–ligand systems is essential to understand a great variety of biological processes that are driven by cellular activity. Although the interactions taking place inside the biological systems are usually intricate and complex, having a preliminary knowledge of the mechanism of binding and the forces involved is a massive step forward in the characterization of these processes [1–3]. In this sense, *in vitro* and *in silico* assays are notably helpful in the designing and discovering of new drugs.

Proteins are large biomolecules which, by nature, present an exceptional structural and topological richness. Under different conditions, they can fold or completely reorganize and generally, in the human body, they fulfil their functions in a highly heterogeneous environment, consisting of varied concentrations of several molecular entities like ions or cells. The balance in this diverse atmosphere is sustained by innumerable interactions and reactions, most of which are controlled by electrostatic and entropic forces [4,5]. Particularly, lysozyme (N-acetylmuramide glyconohydrolase) is one of the notable proteins that are present in a great number of biological fluids and tissues such as tears, saliva, liver blood or lymphatic tissues of humans and other animals [6,7]. It is an antimicrobial globular protein formed by 129 amino acid residues containing six tryptophan (trp), three tyrosine (tyr), and four disulfide bridges [8]. One major peculiarity of this protein is its ability to damage bacterial cell wall by cleavage of β-linkages between the N-acetyl-muramic acid and N-acetyl glucosamine of the peptidoglycan [7], so it takes a huge part in the first barrier of biological defense and can be taken as an essential component of the innate immune system [9]. Also, its well-proven anti-inflammatory, antihistaminic, antiviral and anti-tumor effects have positioned Lysozyme as a reference in the pharmaceutical and food areas. Further, monomeric lysozyme is relatively small, abundant, it presents the ability to carry endogenous and exogeneous substances and it has high stability. This set of attributes makes this biomolecule an outstanding model protein for studies that deal with dynamics, protein folding or ligand interactions [8,10,11].

Likewise, lysozyme has been demonstrated as an effective carrier in drug delivery systems [12,13]. In this line, the present contribution deals with the characterization of the union between the protein and two widespread used β-penicillin: cloxacillin and dicloxacillin. As the efficiency of drugs and their cellular metabolic pathways mostly depend on the interaction with proteins, understanding the forces involved in the complex formation becomes

* Corresponding author.
E-mail address: juanm.ruso@usc.es (J.M. Ruso).

https://doi.org/10.1016/j.molliq.2022.119081
0167-7322/

paramount. For their part, the two antibiotics chosen for the present study are commonly used for the treatment of different infections. Nevertheless, their efficacy is hindered by the β-lactamase resistance that is arising from inappropriate use and propagating fast among pathogenic bacteria. That's why in the recent times novel alternatives are emerging to impair the bacterial resistance and restore the efficacy of old antibiotics [14,15].

From the theoretical perspective, the two antibiotics have an interesting molecular nature, as the only variation in their structure is an additional chlorine atom on the phenyl ring of dicloxacillin. This fact allows to evaluate and compare the different behavior of the two molecules and to investigate the relationship between the intermolecular interactions and the molecular structure [16]. In previous works, this correlation between the architecture and the physicochemical properties were investigated. It was demonstrated that, over a given concentration, both penicillins form small aggregates in aqueous solution [17]. The stability of mentioned aggregates has a massive effect on the bacterial activity [18] and on protein interactions, as it was proven the formation of IgE antibodies resulting from the penicillin haptenation to serum proteins [19,20]. In other studies [21], the interactions of both cloxacillin and dicloxacillin with fibrinogen were assessed in order to evaluate the potential hematotoxicity (off-target fibrinolytic interactions) as hemolytic anemia caused by intravascular hemolysis, and blood clotting disorders-mediated fibrinolysis (*i.e.*, by interactions with the fibrinogen molecule). From the results it was concluded that the semi-synthetic incorporation of the additional Cl atom in dicloxacillin, and its relative docking-pose orientation in the fibrinogen E-region could significantly reduce the appearance of potential fibrinolytic side-effects. Also, the relevant role that the ligands' structure plays in the binding process was confirmed by quantitative calorimetric results.

Following this line and in order to better comprehend the interactions involved in biomolecule-antibiotic systems, a combination of computational and experimental methods was used. Steady state spectroscopic techniques were performed to determine the stoichiometry, the type, and the mechanism of the binding where the quenching of the thryptophanyl fluorescence of the lysozyme has been noted to determine the binding strength. Thermodynamic parameters have been obtained from van't Hoff's relationship, both in temperature dependent fluorometric assays and in titration calorimetric measurements too, conducted to find out the nature of the binding forces and the energies. Concerning the computational studies, in the recent times molecular docking approach is gaining more and more recognition as a powerful tool in rational drug-design [22]. It is very helpful to simulate and model the interaction between a macromolecule and a small ligand at the atomic level. Thus, its utility to interpret many important biological processes becomes evident [23]. Related to this, is the evolution that computational methods have experienced lately. This development allows to obtain more concise, precise and reliable results which conduces to new and more consistent interpretations [24,25].

In view of the foregoing, the objective of the present contribution is to deepen into the thermodynamics and structural features of the lysozyme-penicillin interactions, providing a global and clearer interpretation of the interaction phenomena.

2. Materials and methods

2.1. Experimental procedures

2.1.1. Reagents

Sodium cloxacillin [5-methyl-3- (o-chlorophenyl)-4-isoxazolyl penicillin], sodium dicloxacillin [3-(2,6-dichlorophenyl)- 5-methyl-4-isoxazolyl penicillin] and Lysozyme from chicken egg white, (lyophilized power, protein ≥ 90%, ≥ 40,000 units/mg) were purchased from Sigma-Aldrich and used without further purification. Samples were freshly prepared for each experiment within 1 h. prior to usage. Solutions were made using triple-distilled and degassed water.

2.1.2. Isothermal titration calorimetry

Isothermal titration calorimetry experiments were carried out using a VP-ITC microcalorimeter (MicroCal Inc., Northampton, U. S.) [26] at a temperature of 298.15 K. In each experiment, calorimetric cell (1.4166 mL) was filled with the lysozyme protein solution (0.05 mM) and the β-lactam antibiotic drugs were introduced into the syringe needle (296 μL). Stirring was maintained constant at 416 rpm through all the experiments to assure homogeneity. Before each experiment, 1 h was waited to assure power base line stabilization. 21 injections of 10 μL at a constant rate of 0.5 μL s^{-1} were added every 300 s. A reference power of 15 μJ s^{-1} was applied to guaranty that the signal was not affected by overcompensation mechanism. Dilution heats of pure lysozyme were subtracted systematically from those obtained for the protein–ligand systems in order to assure that all the heat was caused by the binding process alone.

2.1.3. UV–vis absorption spectra

UV–vis absorption spectra measurements were performed on a Cary 100 Bio UV–Vis Spectrophotometer. The spectral range analyzed was 240–400 nm. The reference solution used in the UV measurements was a 0.286 g/L Lysozyme aqueous solution, which corresponds to a concentration of 0.02 mM. Cloxacillin and dicloxacillin solutions were added from 0.0 mM to 1.0 mM at increasing concentrations of (0.1 mM) while maintaining the Lysozyme concentration constant.

2.1.4. Fluorescence measurements

Fluorescence emission spectra were recorded on a Cary Eclipse spectrofluorometer. The excitation and emission splits were 5 nm. The synchronous fluorescence spectra were recorded by adjusting the data interval at 1 nm and the average time at 0.5 s. The range chosen for the analysis was 240–450 nm. Excitation wavelength was set at 280 nm. The fluorescence spectra of Lysozyme- β-lactam antibiotic systems were recorded at 298, 310 and 315 K. Lysozyme concentration was fixed at 0.02 mM and drug solutions were added, from 0.0 mM to 1.0 mM. Inner filter effects were corrected for the quenching experiments using the expression: $F_{corr} = F_{obs} exp\{(A_{exc} + A_{em})/2\}$; where A_{exc} and A_{em} are the absorption of the systems at the excitation and the emission wavelength, and F_{corr} and F_{obs} the corrected and observed fluorescence intensities, respectively. UV–Vis-IR Spectral Software (FluorTools) was utilized for data treatment and processing [27,28].

2.2. Computational procedures

2.2.1. Molecular docking approaches

To address the conformational binding mechanism of lysozyme interacting with the two penicillin antibiotics drugs (*i.e.*, cloxacillin and dicloxacillin) a computational study based on molecular docking simulation was carried out. To this end, as a first step we prepared the lysozyme receptor file stored from the *RCSB Protein Data Bank* (PDB) X-ray structures - *i.e.* with *PDB ID*: 1HER [29]. Afterwards, the lysozyme receptor crystallographic structure as.pdb model was properly optimized by applying the AutoDock Tools 4 software [30]. This procedure starts by removing all the crystallographic water molecules as well as all co-crystallized ligands embedded in the receptor structure, if any. Next, H-atoms are included in the 3D-structure of the lysozyme, followed by an

appropriate hybridization geometry which adds the corresponding partial atomic charges and simultaneously set the protonation states of the X-ray lysozyme.pdb model [31]. Concerning the penicillin antibiotics under study, both ligands were retrieved from the *Pubchem Data Base Chemical Structure Search* as cloxacillin (PubChem CID: 6098; MF: 435.9 g/mol) and dicloxacillin (PubChem CID: 18381; MF: 470.3 g/mol). The procedure of ligand preparation for both penicillin antibiotics was performed using geometry optimization applying MMFF-ligand with the MOPAC extension based on NDDO approximation [32]. Then, in order to explore the antibiotics conformational docking mechanisms with the lysozyme receptor, we applied the well-stablished Vina scoring function developed by Trott *et al.* [30] to achieve the free energy of binging (FEB, kcal/mol) by determining approximated and standard chemical potentials as the sum of force-field interactions terms (*i.e.*, van der Waals, hydrogen bounds and electrostatic interactions). It is important to note that, before the docking simulations, the main lysozyme binding-site was properly predicted through the ezPocket tool [33,34]. The binding site volumetric map of the lysozyme receptor was generated joint to the Cartesian *XYZ*-coordinates which offers the three-dimensional discrete space for setting the docking box simulations [35], *i.e.*: grid box size with dimensions of X = 20 Å, Y = 20 Å, Z = 20 Å and grid box center X = 3.27 Å, Y = 24.19 Å, Z = 27.15 Å, with volume equal to 431.26 Å^3. Next, the accuracy of the docking was set at 50 and for this instance, the best antibiotic conformational binding pose was selected from both drugs (cloxacillin and dicloxacillin). In this context, the affinity (*i.e.*, FEB values for the obtained docking complexes) were categorized as conformationally-unfavorable when the FEB of lysozyme-antibiotic complexes ≥ 0 kcal/mol, thus pointing either extremely low (or complete absence of affinity); otherwise the lysozyme-antibiotic docking complexes were classified as stable from the conformational docking affinity point of view.

2.2.2. 2D Lig-Plot interaction diagrams

This method was performed to determine and identify the different types of docking interactions of the two evaluated penicillins under the interaction with the lysozyme receptor, as well as their contributions from the conformational point of view in the generated complexes. Here, to get the relevant intermolecular interactions between penicillins and the lysozyme receptor, the 2D Lig-Plot interaction diagrams were obtained for both penicillins (cloxacillin and dicloxacillin) only considering the best-ranked conformational binding pose with the highest affinity for each one. To this end, the software Discovery Studio was used. This software is able to identify and visualize the relevant non-covalent inter-molecular interactions present in a given lysozyme-penicillin docking complex automatically generating a 2D-interaction diagram which includes hydrophobic van der Waals interactions, H-bonds, electrostatics, and Π-Π stacking interactions and its corresponding interatomic distances (d_{ij}) for each penicillin binding-pose [36].

2.2.3. Conformational network models with allosteric signal propagation analysis

The present approach offers a conceptual vision on the conformational local and global perturbations induced by the antibiotic ligands over lysozyme receptor in the most relevant conformational state based on the low-frequency normal modes which are directly associated to the intrinsic conformational dynamics and biochemical function of the lysozyme. For this purpose, we selected three representative low-frequency normal modes (*i.e.*, conformational transitions) affecting the global dynamics of the main lysozyme binding site previously predicted, allowing to scan critical Markov conformational states from close-to-open lysozyme binding site conformations, and considering the cited states for the docking simulation conditions as unbound (*i.e.*, theoretical physiological condition) and bound state (*i.e.*, under interaction with the cloxacillin and dicloxacillin). In this context, the local and global perturbations in the allosteric signal propagation are defined by the topological network-based conformational connectivity of the lysozyme measured by the rigidity index and flexibility index which determine the collective anisotropic fluctuations across the different binding states. Herein, deformations in the intra-segment Cα-Cα atomic residue in the conformational network were evaluated for the unbound and bound states (*i.e.*, cloxacillin and dicloxacillin) which could be biochemically relevant (*i.e.*, as in the case of physiological unbound state of the lysozyme binding site) or unfavorable from structural point of view by affecting the allosteric signal propagation of lysozyme binding site native conformation and its function under interaction with the penicillin drugs. Find more details in the Figure SM1 as supplementary material. Here, the allosteric signal propagation in the lysozyme is fully defined by the 3 $N \times 3$ N Hessian matrix ($H_{i,j}$) that can reproduce the signal propagation efficiency in the lyzosyme residue network [37], and in which its N-elements ($1 \leq i, j \leq N$) are the second derivatives of the anisotropic network potential ($V_{R\_receptor}$ or $V_{R\text{-}L\_receptor+ligante}$) that describes the (3 N)-XYZ-displacements $N \in \mathbb{R}^3$ as ($\Delta R_{ij} = R_{ij} - R_{ij}^0$) of all the (i,j)-residue pairs sensors (i) and effectors (j) of lysozyme receptor in N-blocks of dimension 3 each, and where $\gamma = 0.5$ is an elastic deformation constant, in absence (lysozyme unbound state) and under interactions (lysozyme plus cloxacillin or dicloxacillin as bound state) as represented in the equations [38–40]:

$$V_{(lysozymeunbound)} = \sum_{(i<j)\in N(R)} \frac{1}{2}\gamma_R\left(R_{ij} - R_{ij}^0\right)^2 \quad (1)$$

$$V_{(lysozyme+penicillins)} = \sum_{(i<j)\in N(R)\cap N(L)} \frac{1}{2}\gamma_R\left(R_{ij} - R_{ij}^0\right)^2 + \sum_{(i<j)\in N(R,L)} \times \frac{1}{2}\gamma_L\left(R_{ij} - R_{ij}^0\right)^2 \quad (2)$$

3. Results and discussion

3.1. Experimental characterization

Spectroscopic analysis is a well proven tool to evaluate conformational changes in protein–ligand systems. The formation of a complex or the structural changes that may derive from the arrangement of new structures can be deciphered by studying the spectral curves under different conditions and concentrations. Particularly, lysozyme presents three aromatic amino acid residues, tyrosine, phenylalamine and tryptophan, which are the main responsible of its absorption peak. Of the mentioned three, tryptophan is the one whose contribution is stronger, resulting in a peak at 278 nm [41]. Fig. 1 shows the spectral curves of different systems of drug-protein. As both drugs have a maximum absorption peak which is near the one found in the protein, corresponding subtractions of the spectra were performed. In the present case, the peak at 278 nm suffered similar changes for both drugs, slightly diminishing its maximum value with increasing concentrations of the ligand, indicating a raise in the hydrophobity in the surroundings of the aromatic amino acids of the protein [42]. Furthermore, the π-π stacking interaction between the aromatic ring of the antibiotic drugs and the phenyl rings of amino acid residues may be another cause for the hypochromism [7].

To continue the analysis, fluorescence studies were also performed. Usually, protein–ligand interactions cause a change in the intrinsic emission trait of proteins, which is mainly produced

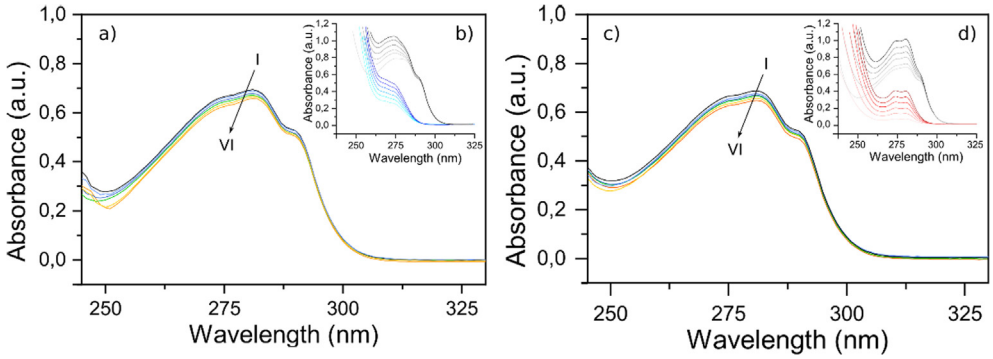

Fig 1. UV absorption spectra of Lysozyme in the absence and presence of a) Cloxacillin and c) Dicloxacillin. Insets: b) Blue: UV absorption spectra of increasing concentrations of Cloxacillin, Grey: UV absorption spectra of Lysozyme (0.02 mM) and increasing concentrations of Cloxacillin combined. d) Red: UV absorption spectra of increasing concentrations of Dicloxacillin, Grey: UV absorption spectra of Lysozyme (0.02) and increasing concentrations of Cloxacillin combined. $C_{lysozyme}$ = 0.02 mM; C_{Clox} (x 10^{-1}) (I-VI) = (0, 2, 4, 6, 8, 10) mM; C_{Diclox} (x 10^{-1}) (I-VI) = (0, 1, 2, 3, 4, 5) mM.

by the presence of the tyrosine (Tyr), phenylalanine (Phe) and tryptophan (Trp), residues. Among them, when the protein solution is excited at 280 nm or more, the fluorophores with the most important contribution are Trp-62 and Trp-108, ubicated at the substrate binding sites [43].

Quenching of a fluorophore with the addition of a ligand can be classified in three different types: collisional, static, or combined quenching process [44,45]. When an excited state fluorophore gets neutralized by a quencher, we talk about collisional quenching. Instead, static quenching involves the development of ground state non-fluorescent complexation, and it does not depend on diffusion and molecular collision. For its part, combined quenching is caused by both collision and complex formation with the same quencher [46,47]. The fluorescence spectra of lysozyme in the presence of different concentrations of drugs at 25 °C and 280 nm are given in Fig. 2. The fluorescence emission spectrum of the protein alone presents a peak at around 340 nm, which is attenuated with the sequential addition of both ligands. As cloxacillin and dicloxacillin have a minor but not negligible absorption from 200 to 400 nm, the fluorescence spectra were corrected for the inner filter (see *Materials and Methods: Fluorescence measurements).*

In order to describe the quenching process, the well-known Stern-Volmer equation is usually used, which allows to identify if the mechanism corresponds to a dynamic, static or mixed process [47]:

$$F_0/F = 1 + K_{sv}[Q] = 1 + k_q\tau_0[Q] \quad (3)$$

where F_0 is the emission intensity of lysozyme in the absence of drugs and F is the intensity when a certain concentration of antibiotic is added. K_{sv} is the Stern-Volmer quenching constant, [Q] is the concentration of the drugs, k_q is the quenching rate constant of the protein and τ_0 is the average lifetime of the biomolecule, taken as 5.9×10^{-9} s for lysozyme [48]. Values of Stern-Volmer constants (K_{SV}) can be calculated from the linear plots of F_0/F versus the quencher concentration [Q], as shown in Fig. 2.

A Stern–Volmer plot of F_0/F against [Q] is linear for purely dynamic (K = 0) or purely static (k = 0) quenching but curved upwards for combined quenching. In this line, a curvature of a Stern–Volmer plot usually designates combined quenching. Plots obtained for the present cases are shown in Fig. 3. For both drugs, and at different temperatures, a linear correlation can be noticed, suggesting that there is no coexistence of interactions occurring between Lysozyme and cloxacillin or dicloxacillin. Analyzing this condition and the obtained values of k_q, the type of quenching can be deducted and is usually considered a good primary observation for determining the quenching implicated in the interaction between proteins and ligands [49]. For dynamic quenching, when the interaction is mostly diffusion-controlled, the values of k_q are in the range of 1×10^{10} M^{-1} s^{-1}. For values higher than the diffusion-controlled limit, the quenching type corresponds to a static one. As shown in Table 1, in the interaction between cloxacillin and dicloxacillin with lysozyme at 25 °C, the quenching rate constant is around 10 times the maximum diffusion rate limit, which is a robust sign that the quenching involved is a static one in both systems. Furthermore, static and dynamic quenching are inversely related to changes in temperature. While a rise in temperature is

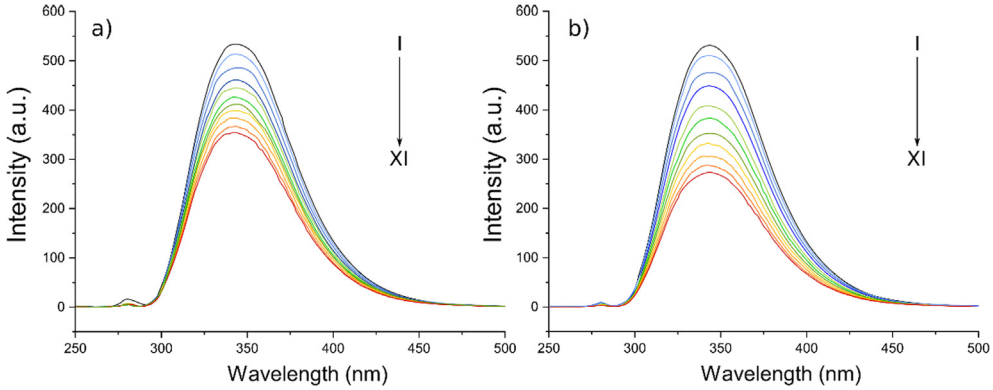

Fig. 2. Fluorescence emission spectra of Lysozyme in the absence and presence of different concentrations of a) Cloxacillin and b) Dicloxacillin at λ_{ex} = 280 nm, T = 298 K. $C_{lysozyme}$ = 0.02 mM; C_{Clox} (x 10^{-1}) (I-XI) = (0, 1, 2, 3, 4, 5, 6, 7, 8, 9, 10) mM; C_{Diclox} (x 10^{-1}) (I-VI) = (0, 1, 2, 3, 4, 5, 6, 7, 8, 9, 10) mM.

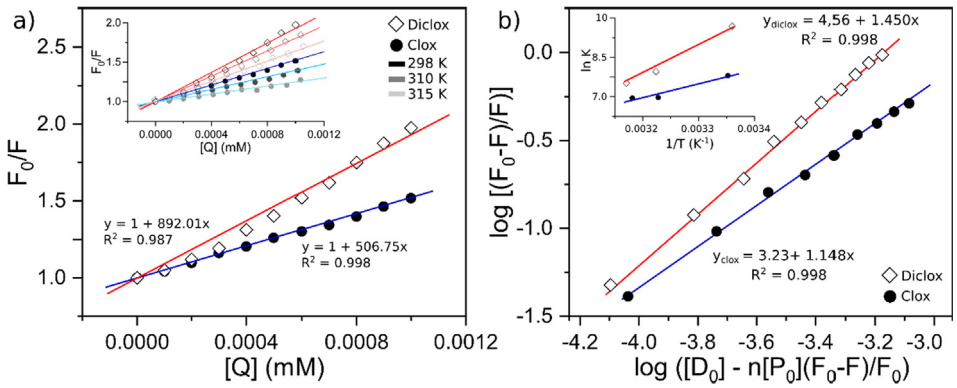

Fig. 3. (a) Stern-Volmer plots for the quenching of Lysozyme by Clox (●) and Diclox (◆). Inset: Quenching at different temperatures (298, 310, 315 K). In blue colors are represented the fittings corresponding to cloxacillin, in red, corresponding to dicloxacillin. CLysozyme = 0.02 mM. (b) Plots of log[(F_0-F)/F] vs $\log\left\{[D]_0 - n\frac{[P]_0(F_0-F)}{F_0}\right\}$. Inset: van't Hoff plot of lysozyme interaction with Clox (●) and Diclox (◆).

Table 1
Stern-Volmer quenching constants and binding parameters for the interaction of lysozyme with Cloxacillin and Dicloxacillin at 298 K.

	Stern-Volmer quenching constants			Binding parameters		
	10^{-2} Ksv (mol^{-1})	10^{-10} kq (mol^{-1} s^{-1})	R^2	n	10^3 K_A (mol^{-1})	R^2
Clo	5.07 ± 0.09	8.59 ± 0.03	0.998	1.15 ± 0.01	1.66 ± 0.01	0.998
Diclo	8.92 ± 0.13	15.12 ± 0.06	0.987	1.45 ± 0.01	36.47 ± 0.03	0.998

always positive for dynamic quenching, static type processes get favored when decreased. Consequently, fluorescence measurements were also carried out at 37 °C and 42 °C. Resulting regressions are presented in the insets of Fig. 3. As expected, values of K_{SV} decreased on increasing temperatures, confirming the involvement of static quenching. From a structural point of view, this means that the quencher (penicillin) and the fluorophore (protein residue) are so close to each other that the pair touch before light excitation, resulting in a nonfluorescent complex [50].

Regarding the binding and thermodynamic parameters, the number of binding sites (n) and the association constant (k_A) are crucial characteristics of the protein–ligand interactions. As a formation of non-fluorescent complex was considered between the protein and both drugs, for the binding interactions an equilibrium should be assumed [51]:

$$P + nD \rightleftharpoons P - D_n \tag{4}$$

Being, n the number of binding sites, P the protein and D the drug or, generally speaking, the ligand. The equilibrium constant is given by:

$$k_A = \frac{[P - D_n]}{[P][D]^n} \tag{5}$$

$[P - D_n]$ is the equilibrium concentration. Considering that the complex and drug are non-fluorescent, we have that:

$$[P]_0 = k \times F_0, \tag{6}$$

$$[P] = k \times F \tag{7}$$

$$[D] = [D]_0 - n[P - D_n] \tag{8}$$

Being $[P]_0$ the total concentration of protein (0.02 mM) and $[D]_0$ the total concentration of drug, so:

$$k_A = \frac{[P]_0 - [P]}{[P]\{[D]_0 - n([P]_0 - [P]} \tag{9}$$

$$\log\frac{[P]_0\text{-}[P]}{[P]} = \log k_A + n \cdot \log\{[D]_0 - n([P]_0 - [P])\} \tag{10}$$

$$\log\frac{F_0\text{-}F}{F} = \log k_A + n \cdot \log\left\{[D]_0 - n\frac{[P]_0(F_0 - F)}{F_0}\right\} \tag{11}$$

Where F_0 and F are the same as in Eq. (3).

From the linear plot of $\log\{(F_0 - F)/F\}$ versus $\log\left\{[D]_0 - n\frac{[P]_0(F_0-F)}{F_0}\right\}$(Fig. 3), values of $\log K_A$ and n are obtained. The average binding site number (n) is close to 1 in both systems, being 1.15 ± 0.01 for cloxacillin and 1.45 ± 0.01 for dicloxacillin which is indicative of a single binding site for both drugs to the biomacromolecule. For its part, values of the binding constant are in the order of 10^3 and 10^4 for cloxacillin and dicloxacillin respectively, indicating that affinity is moderate but significantly higher for the later.

Thermodynamics also provide a deeper insight into the mechanisms involved in the process. Mostly, the binding between a ligand and a protein occurs via noncovalent interactions; generally involving hydrogen bonding, hydrophobic forces and electrostatic interactions [52]. To elucidate the contribution of these interactions, the van't Hoff equations can be used:

$$\ln K = -\Delta H/RT + \Delta S/R \tag{12}$$

ΔH is the enthalpy change, which in the range of temperatures studied, is assumed to be constant and ΔS is the entropy change. Then the free energy change (ΔG) of the binding process can be obtained as $\Delta G = \Delta H - T\Delta S$.

Attending to the sign of the thermodynamic parameters, the principal binding forces involved can be determined as follows: if ΔH and ΔS are both positive, the binding corresponds to hydrophobic forces, if both are negative, the major forces involved are van der Waals and hydrogen-bond formation, and if ΔH is negative while ΔS positive, the interactions are of the electrostatic/ionic type [53]. In the present case both thermodynamic parameters presented negative values (inset Fig. 3), hence it can be safely

inferred that the van der Waals and hydrogen bonding are the main responsible of the interactions for both drugs.

Deepening into the thermodynamic characterization, the interaction of drugs and lysozyme can be also assessed by means of isothermal titration calorimetry (ITC) technique. ITC is an especially useful tool to describe the calorimetric aspects of the binding and consequently the type of bonding [54]. Normally, in titration tests, small aliquots of ligand are injected through a syringe needle into a calorimetric cell filled with the macromolecule solution. Each injection has an associated energy deflection which can be endothermic or exothermic depending on the system and the molecules involved. In the present case, Fig. 4, heat deflection has a negative nature, indicating that the reactions taking place are exothermic. Likewise, the negative peaks also underscore the fact that lysozyme protein is not suffering major conformational changes. Here, the concentration selected for the protein solution was 0.05 mM and around twenty times higher for drug solutions, in order to assure complete saturation. As it can be seen in the graphs, assays performed with cloxacillin and dicloxacillin presented different patterns, pointing out that both binding processes followed similar but non-identical paths. At a first glance, in the case of dicloxacillin interaction seems to be more constant and immediate while for cloxacillin the reaction takes place sharply after a specific concentration. Furthermore, in view of the results, protein–ligand reaction is more favorable for dicloxacillin, as heat deflections are higher, and the saturation occurs at bigger molar ratios. These first impressions are in great accordance with previous conclusions draw from spectroscopic analysis.

For a more complete description of the thermodynamics of the systems, ITC results were fitted to standard non-linear least-squares regression, revealing that for both drugs the binding stoichiometry (n) was close to 1, as they interact with lysozyme binding site at 1:1 M. For the binding constants (K), values were at the order of $\sim 10^2$, meaning that the interaction exists but is moderate. The obtained thermodynamic parameters accompanying the lysozyme-penicillin interactions showed a negative enthalpy and entropy changes with values of ΔH = -9.83 kcal/mol, ΔS = -9.73 cal/mol for cloxacillin and ΔH = -10.91 kcal/mol, ΔS = -11.74 cal/mol for dicloxacillin. Thus, the free energy of binding results ΔG = -6.93 kcal/mol and ΔG = -7.41 kcal/mol for cloxacillin and dicloxacillin, respectively. Once again, thermodynamic parameters followed a similar pattern for the two β-lactam antibiotics: the enthalpy and entropy change have negative values, so van der Waals, hydrogen bonds and hydrophobic forces are the mainly contributors to the interaction. At pH 8.5, the fraction of non-ionized molecules of cloxacillin and dicloxacillin in which the carboxyl group is not dissociated is 5.5% [55]. Thus, some of the molecules present neutral charges that avoid them to interact electrostatically with lysozyme, hampering the reaction and lowering the enthalpy values. For its part, negative entropy changes are synonym of hydration and loss of conformational freedom as a consequence of complex formation [56]. Taking into consideration that the protein–ligand binding and the β-lactam antibiotic self-aggregation process [17] follow a similar comportment, it is safe to assume that there is no desolvation present in the interaction. Therefore, entropy changes are primarily caused by alterations of the conformational flexibility of lysozyme and under the interaction with the antibiotics (See Figure SM2), changes in translational and rotational degrees of freedom and reorganization of their solvation shells.

When comparing results for cloxacillin and dicloxacillin, once again values show that the former has a higher affinity, and the interaction seems more robust. One possible explanation for this disparity is the presence of a second Cl atom in a meta position of the dicloxacillin molecule. This atom could function as an anchor between protein and ligand, facilitating the existence of halogen bonding. This fact would contribute to a closer interaction and to the stabilization of the complex. Moreover, it has also been probed that aromatic halogen substitutions can alter the geometries and the σ-hole characteristics of the formed complexes, by means of secondary interactions [57,58] and modifications in the position of these halogen substitutes can contribute to notable variations in binding thermodynamic parameters [59].

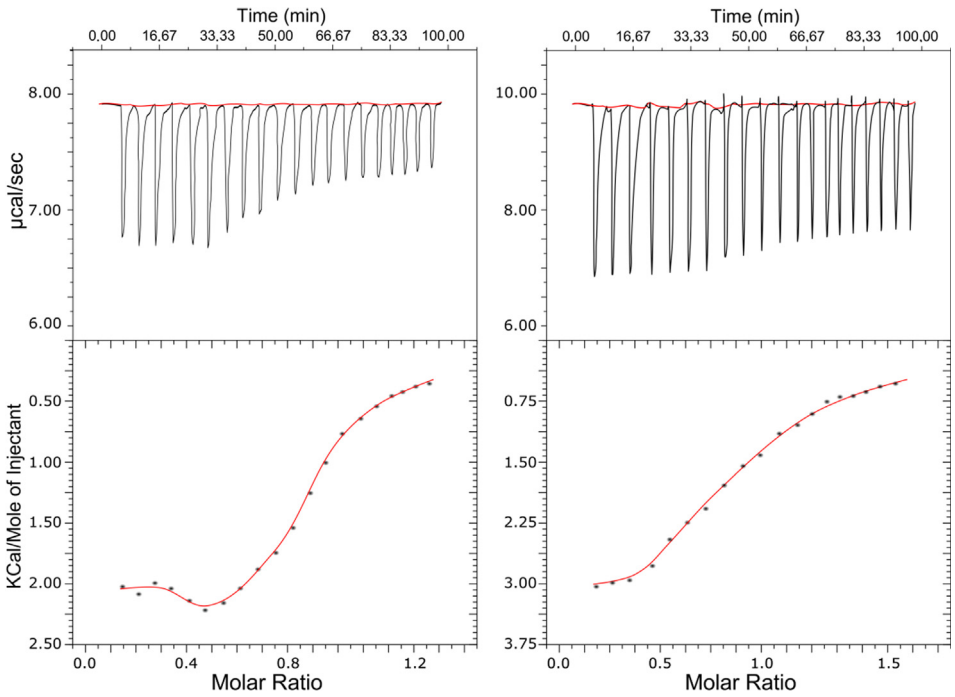

Fig. 4. Heat of interaction. ITC results for titration of: (Left) Cloxacillin (1 mM) and (Right) Dicloxacillin (1.2 mM) into Lysozyme solution (0.05 mM) at 298.15 K. Each dot represents a 10 µL injection.

3.2. Computational characterization

3.2.1. Molecular docking coupled with conformational network analysis

Herein, the molecular docking results are presented in the Fig. 5 for both penicillins docking complexes with the corresponding 3D-conformational network of interactions as cloxacillin/lysozyme (Fig. 5; A and B) and dicloxacillin/lysozyme (Fig. 5; C and D). The accuracy of our docking approach was ensured by performing a proper prediction of the binding-site of lysozyme with an optimal druggability for binding both penicillin antibiotic drugs and with the best docking root mean square deviation (R.M.S.D; Eq. (13)) for all the crystallographic docking poses which was stored as a criterion of correct docking pose accuracy for atomic positions below 2 Å [60].

$$RMSD = \sqrt{\frac{\sum_{i=1}^{n_L}\sum_{j=1}^{n_P}(x_i - x_j)^2 + (y_i - y_j)^2 + (z_i - z_j)^2}{n_L \times n_P}} \quad (13)$$

In Eq. (13), n_L is the number of atoms of the ligand and n_P is the number of atoms of the lysozyme. Additionally, each term included in the double summation represents the distance between a ligand (*i.e.*, (i)-atom belonging to cloxacillin or dicloxacillin) with Cartesian coordinates (x_i, y_i, z_i) and a j-atom from the lysozyme atom with Cartesian coordinates (x_j, y_j, z_j). To do this, in the present study the main lysozyme binding pocket was predicted by using an *ezPocket* tool and visualized as 3D-van der Waals surface concave region (Fig. 5; A and C) forming a stable thermodynamics docking complex with both penicillin drugs with very close Gibbs free energy value of ΔG (clox./lysozyme) = -7.7 kcal/mol (RMSD = 1.071 Å) and ΔG (diclox./lysozyme) = − 7.5 kcal/mol (RMSD = 1.0 86 Å). For this instance, the best-ranked binding-conformation adopted by the cloxacillin and dicloxacillin into the lysozyme-binding site was modeled for both penicillin drugs considering the Markov conformational "state 1" that fits very well with the highest affinity in the pseudo-open conformation of lysozyme binding pocket. From the numerical point of view, these values are in perfect agreement with those obtained experimentally (see ITC section). However, experimentally, the interaction with dicloxacillin is the most favorable, while computationally, the obtained values for both penicillins are really close.

Following the theoretical results, we strongly suggest that, in general terms the penicillins can interact in the predicted binding site placed in the middle of the lysozyme receptor according to a spontaneous thermodynamics process with both ligands (*i.e.*, cloxacillin and dicloxacillin). Particularly, we identify a predominance of hydrophobic non-covalent binding events with significant number and variety of aromatic π-π stacking interactions (ex., π-sigma, π-alkyl, π-anion, π-sulfur) in both penicillin drugs. For the case of cloxacillin drug, its relative affinity (ΔG = − 7.7 kcal/mol) greater respect to the dicloxacillin with affinity of −7.5 kcal/mol suggests that in the cloxacillin drug this fact could be directly attributed to the presence and additional thermodynamic contributions of halogen-bound interactions of the Cl atom belonging to the cloxacillin which interacts with the residue Ala107 and also by the strong stabilization provided by the presence of three conventional H-bound interactions of cloxacillin with Trp63, Asp101 and Ala107 in the cloxacillin/lysozyme docking complex, which are totally absent in the case of the dicloxacillin/lysozyme complex. Herein, it is important to note that the presence of Pi-sulfur (with the lysozyme Asp52 residue) and Pi-anion interactions (with the lysozyme Trp63 residue) identified in the dicloxacillin/lysozyme complex provide a lesser thermodynamic contribution to the affinity when compared with the Cl atom halogen-bounds of the cloxacillin.

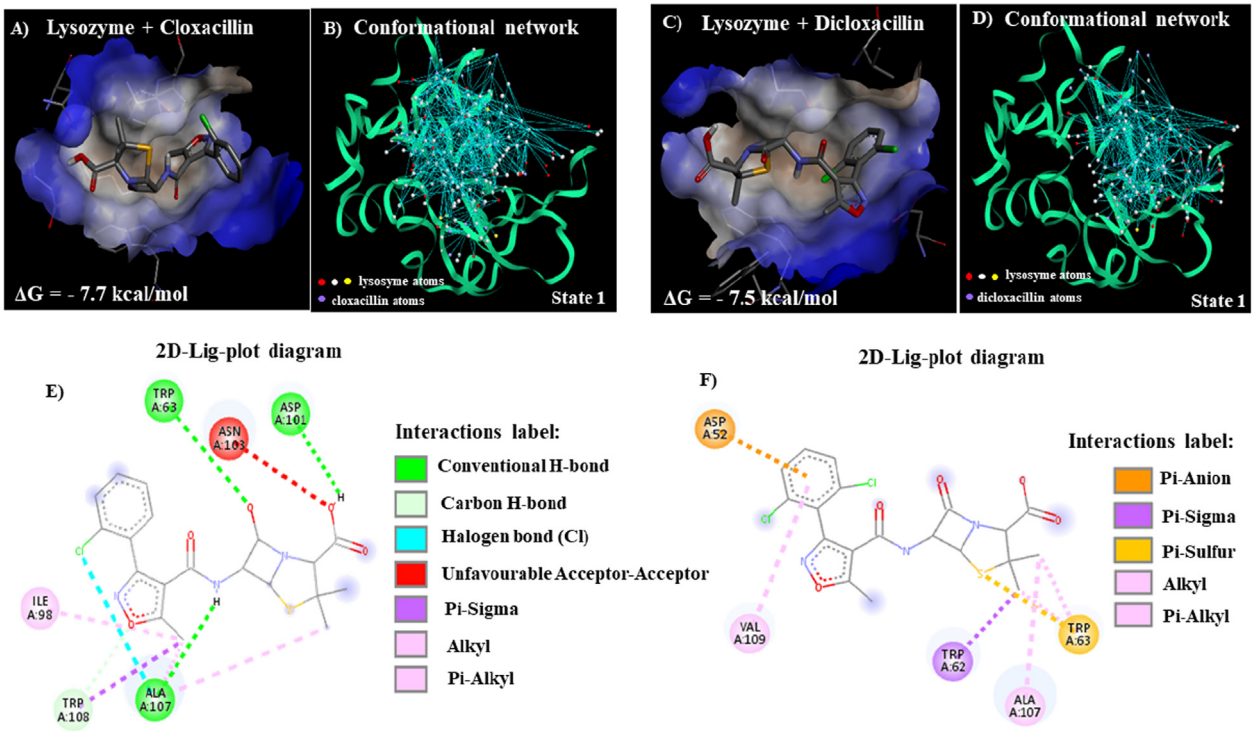

Fig. 5. In the top, Molecular docking complexes with the corresponding 3D-conformational network of interactions are represented as A), B) cloxacillin/lysozyme and B), C) dicloxacillin/lysozyme, respectively. In the bottom E) and F), represent the 2D-lig-plot diagrams of interactions for the best-ranked conformations of the penicillins evaluated in the pseudo-open conformation of lysozyme binding pocket (state1). In addition, the crystallographic validation-based Ramachandran plot was performed for the whole lysozyme structure and individual binding residues to avoid the present of false positives docking results from the structural point of view. See details in **Figure SM3** in the supplementary material.

Because of the differences detected in the topology of the anisotropic conformational network suggesting that the interactions of the cloxacillin and dicloxacillin could affect in a different way the signal propagation and communication efficiency of the lysozyme in the bound state involving additional atoms of the regulatory helix responsible for the opening and closing of the main lysozyme pocket. Please, refer to Fig. 5 B) and D). In accordance with experimental evidence, it is important to note that in general terms the aromatic π-π interactions detected for both penicillins excellently corroborate the resulting absorption peak at 278 nm mentioned above (see UV–vis and fluorescence sections). Besides, the results obtained by using conformational network analysis allow to validate the subtle quantitative differences in the docking results (very close ΔG values for both penicillins).

One of the fundamental challenges, associated with the conformational network analysis, is the extremely high dimensionality of the penicillin-lysozyme conformational space [40,61]. In this regard, to significantly reduce the extremely high dimensionality of the penicillin-lysozyme conformational space during the evaluation of of allosteric signals propagation we focus only in the most dominant normal mode (normal mode 1) of the lysozyne which corresponds to the low frequency mode highly relative to the biological catalytic function of the enzyme and regulates large-scale allosteric signal propagation in both, the unbound and bound states (*i.e.*, under penicillin docking interactions). It is well-known that fast-frequency modes only affect or are restricted to local region of the proteins (*i.e.*, lysozyme) (*i.e.*, ranging from the mode 7 to 20, Refer to **Figure SM4 A-C** in the supplementary material).

Particularly, the conformational differences between the two penicillins within the lysozyme binding pocket could be associated to small differences generated under perturbed conditions, showed as different elastic deformations-induced by the two penicillins in the local architecture (network topology of elastic normal mode), intrinsic conformational dynamics, and signal propagation in the residue network of the lysozyme compared with the unperturbed (*i.e.,* native conformation in the absence of penicillin). Particularly, we identify notable differences in the patterns of signal propagation for the three simulation conditions evaluated, as represented in the Fig. 6**.**

The behavior of the allosteric signal propagation response of (*i*)-lysozyme effector residues provides relevant information regarding the effective communication distances for intra-segment Cα-Cα atomic distances, which can be classified into the following categories depending on the distance at which the signals appear from the lysozyme binding site (covering from Ser50 to Leu75) as: *i)* short distance propagations (10–22 residues), *ii)* medium distance propagations (23–26 residues), and *iii)* long distance propagation (27–50 residues). Besides, it is important to consider the signal amplitudes triggered by the lysozyme effector residues. Then, contemplating the obtained results for signal propagation response of lysozyme for the theoretical physiological state (Fig. 6A) compared with the bound states (Fig. 6; B and C) were detected the occurrence of medium-to-long distance allosteric signals propagation starting from the lysozyme binding site and involving different types of effector residues, and also with notable differences in terms of amplitude of the elastic deformations under interaction with the cloxacillin and dicloxacillin. Following this idea, the cloxacillin (Fig. 6B) is able to activate significant effector response with elastic deformation in Ala107, Asp101, Ser36, and Ile98 while dicloxacillin (Fig. 6C) activates the Ala95 (similar to the physiological condition), and additionally activates the Val92, Phe38, Glu35, and Val2. Please, note that both penicillins are able to activate and propagate "abnormal" allosteric signal (or non-physiological signal patterns of propagation) suggesting that lysozyme function could be compromised in the bound state. These allosteric effects could, in fact, have a negative impact in the structure and flexibility properties of the lysozyme binding site. Indeed, the presence of cloxacillin and dicloxacillin in the lysozyme binding site can theoretically affect the low-frequency normal mode of the lysozyme. In this regard, we suggest that, specifically the conformational state 1 (normal mode 1), conformational state 2 (normal mode 2), and conformational state 3 (normal mode 3) are affected by the penicillin interactions, maybe because of the interaction-based modulation of the conformational dynamics of the network of effector residues (Arg45, Asn46, Thr47, Asp48) composing the regulatory alfa-helix (see Fig. 7). In the previous section, when we compared the results of docking and ITC, we commented that there was a certain contradiction as to which penicillin interacts more spontaneously with lysozyme: dicloxacillin according to ITC, and cloxacillin according to docking. We have just seen how the propagation of the allosteric signal produced by penicillins varies considerably. We must take into account that the optimization functions used in docking methods are confined to specific, small-sized areas, while the experimental ITC measurements refer to a global energy process. Therefore, we can consider that the origin of the discrepancy in both hypotheses lies in the fact that the docking methods do not consider the disturbance that the binding process induces in the protein residues far from the pocket.

The allosteric signal propagation analysis, allows the visual representation of the strength of allosteric perturbations by generating the matrix of local and global signals from the cited conformational states and binding conditions (unbound and bound state of lysozyme) [40]. It is well known that lysozyme structural fluctuation, typically is measured by the Debye-Waller B-factors, which in turn is a manifestation of lysozyme flexibility, which strongly correlates to its biochemical function. In this concern, we could note from the conformational results that the collective conformational dynamics of the lysozyme is strictly dependent on the balance of the flexibility/rigidity properties of the lysozyme (*i.e.*, flexibility/rigidity index (FRI) in the whole lysozyme structure). The flexibility-rigidity index (FRI) can be efficiently applied in our study based on the theory of continuum elasticity with atomic rigidity representing a robust multiscale formalism for describing our systems, explained by the main transition conformational states [62]. In this sense, the conformational topological connectivity of lysozyme can be measured using the rigidity and flexibility index. The rigidity index can be tackled considering an N-atom representation of the lysozyme structure under unbound and bound state. Where the coordinates of lysozyme residues (or C(α)-atoms) are given as $\{d_j | d_j \in \mathbb{R}^3, j = 1, 2, \cdots, N\}$. For this instance, we call $||d_i - d_j||$ the Euclidean space distance between the i-th residue and the j-th residue. In addition, a general correlation kernel, Φ ($||d - d_j||; \eta_j$), is a real-valued monotonically decreasing function satisfying the following conditions (Eqs. (14) and (15)).

$$\Phi\left(\|d - d_j\|; \eta_j\right) = 1 like \|d - d_j\| \to 0 \tag{14}$$

$$\Phi\left(\|d - d_j\|; \eta_j\right) = 0 like \|d - d_j\| \to \infty \tag{15}$$

here, η_j is to denotes an atomic type of dependent scale parameter. While the correlation transition matrix (M_{ij}) between the i-th and j-th lysozyme atoms (C(α)-atoms) is given by the Eq. (16):

$$M_{ij} = \Phi\left(\|d - d_j\|; \eta_j\right) \tag{16}$$

The M_{ij} represent a correlation transition matrix (refer to Fig. 7; H, J, and L) which contain relevant information regarding flexibility and rigidity properties of the lysozyme and can be computationally

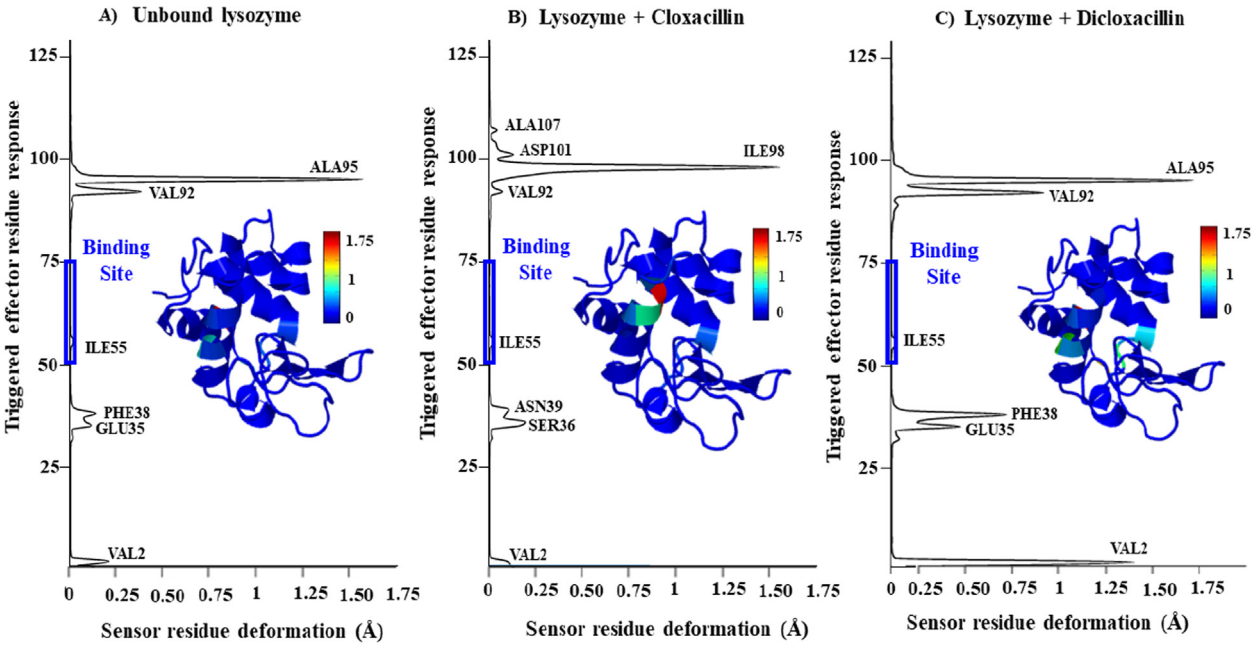

Fig. 6. Graphical representation of the lysozyme signal propagation properties under the three simulation conditions evaluated in the elastic normal mode 1; namely: A) lysozyme unbound state, B) lysozyme plus cloxacillin, and C) lysozyme plus dicloxacillin. The colored structures are based on the size of deformations from the lysozyme-sensor residues (x-axis) and the specific triggered response - *i.e.*, activation of effector residue signals (y-axis). On the right of each graph the 3D-cartoon representations for the simulated conditions are showed with the corresponding color intensity bar where blue-to-yellow labelled regions correspond to weak-to-moderate signal perturbations whereas the labelled regions orange-to-dark red correspond to regions with high propensity to allosteric signal perturbations. The blue rectangle (y-axis) covering from the effector regulatory residue Ser50 to Leu75 is to denote the lysozyme binding site region where the propagation of allosteric signals started. More details about the effector regulatory residue can be found in the **Figure SM5**.

obtained to visualize the connectivity among lysozyme i-sensor and j-effector residues (as C(α)-atoms). We define a position (d) dependent rigidity function $R(d)$ as Eq. (17):

$$\boldsymbol{R}(\boldsymbol{d}) = \sum_{j=1}^{N} w_j \Phi\left(\|\mathrm{d} - d_j\|; \eta_j\right) \tag{17}$$

herein, w_j represents an atom type dependent weight like carbon, nitrogen, sulfur, and oxygen atoms can have different weights. We can apply the generalized equations to stablish the position (d) dependent rigidity function $R(d)$ within the two forms as a generalized exponential function (Eq. (18)) and generalized Lorentz functions (Eq. (19)); respectively as represented below:

$$\boldsymbol{R}(\boldsymbol{d}) = \sum_{j=1}^{N} \Phi\left(\|d_i - d_j\|; \eta_{ij}\right) = e^{-\left(\frac{\|d_i - d_j\|}{\eta_j}\right)^k}, k > 0 \tag{18}$$

$$\boldsymbol{R}(\boldsymbol{d}) = \sum_{j=1}^{N} \Phi\left(\|d_i - d_j\|; \eta_{ij}\right) = \frac{1}{1 + \left(\frac{\|d_i - d_j\|}{\eta_j}\right)^v}, v > 0 \tag{19}$$

Essentially, the correlation between any two atoms of the lysozyme should decay according to their distance as observed in the results obtained for lysozyme signal propagation under the bound state simulation conditions for lysozyme plus cloxacillin, and lysozyme plus dicloxacillin where the effector response signals are express several differences respect to the unbound state (refer to Fig. 6, A, B, and C).

The presence and absence of a given effector residue signal is strongly associated to the lysozyme binding pocket continuity-based descriptor (P_{c_lyso}) [63], which is structurally related to attributes as binding site appearance, merging and volume change in the lysozyme. The continuity descriptor is defined by the Eq. (20):

$$P_{c\_lyso} = \{P_i | P_i \cap P_{ref} > 0\}, i = 1, 2, \cdots, n \tag{20}$$

where, P_{ref} represents the evaluated pocket in the native conformation, P_i corresponds to the *i*-th binding pocket which is spatially overlapped with the P_{ref}, n represents all the potential cavities or pockets, and P_{c_lyso} denotes the binding pocket continuity consecutively assembled pockets. The P_{c_lyso} is strongly depends on the proximity of the neighboring pockets, and on their flexibility properties which are associated to the different conformational states (*i.e.*, state 1, state 2, and state 3) that the pocket can adopt under the presence or absence of ligands (cloxacillin and dicloxacillin) see Fig. 8. Besides, the lack of pocket continuity P_{c_lyso} descriptor can be associated with the decay of signal propagation [64].

With this in mind, likewise, we can define a position (d) dependent flexibility function for the flexibility index (F(d); as the inverse of the function represented in the Eq. (17)) according to the following Eq. (21):

$$F(d) = \frac{1}{\sum_{j=1}^{N} w_j \Phi\left(\|\mathrm{d} - d_j\|; \eta_j\right)} \tag{21}$$

The flexibility index F(d) of lysozyme is directly associated with the Debye-Waller B-factors according to the Eq. (22) and (23) for the unbound and bound simulation condition in a given conformational state σ.

$$B_{lyso} = c \cdot F(d)_\sigma + b; \forall_i = 1, 2, \cdots, N \tag{22}$$

$$B_{lyso} = c \cdot F(d)_\sigma + b + f; \forall_i = 1, 2, \cdots, N \tag{23}$$

where $\{B_{lyso}\}$ represent theoretically predicted B-factors (*i.e.*, lysozyme flexibility), and c and b are two constants to be obtained by simple linear regression. In the Eq. (23), the conformational flexibility-based B-factor (B_{lyso}) is to capture the intrinsic dynamic in the bound state under the action given force (f) representing the perturbations induced by the penicillins (*i.e.*, cloxacillin and dicloxacillin) in the main lysozyme binding site.

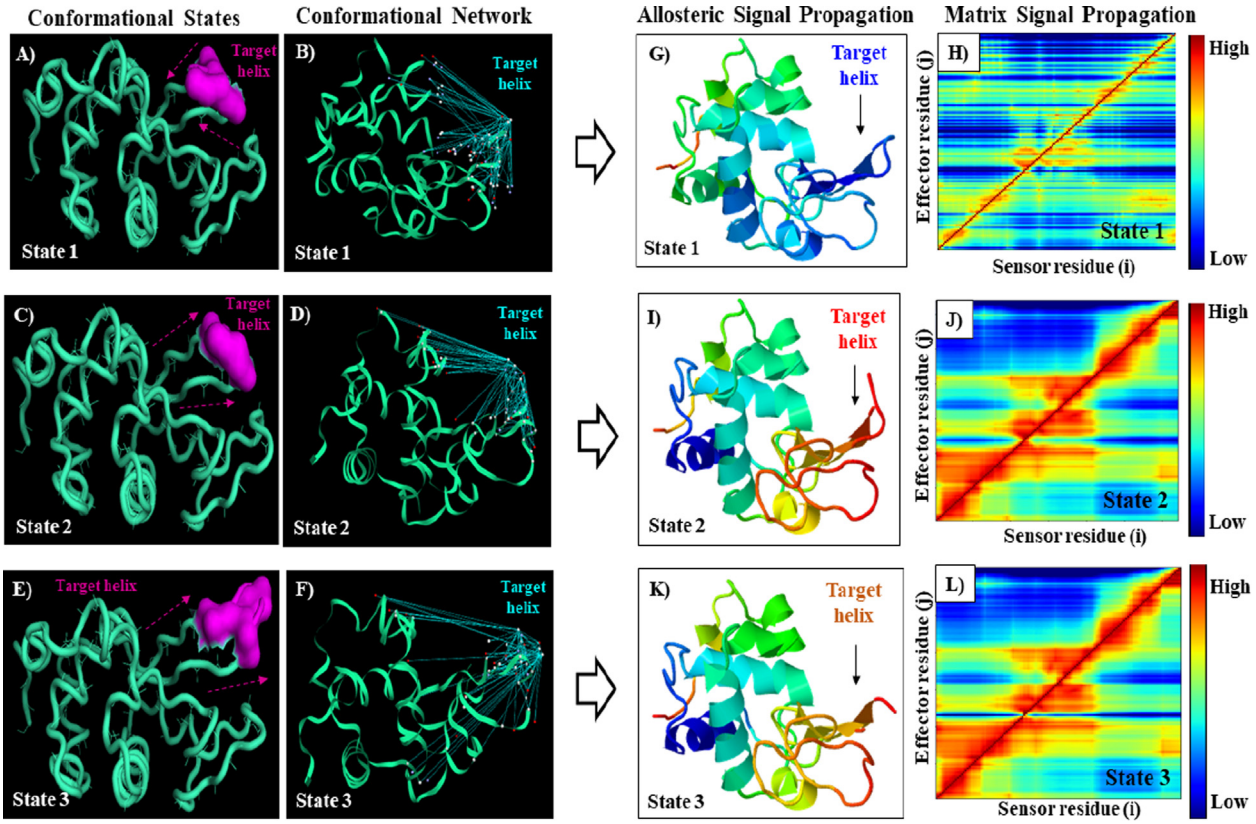

Fig. 7. In the right (A-F), graphical representation of the lysozyme 3D-structure highlighting the regulatory alfa-helix (labelled-purple) with the corresponding 3D-conformational network from the conformational state 1 to 3 (normal mode 1 to 3). Herein, the purple arrows are to indicate the movement direction of the target-alfa helix from pseudo-open (state 1) to fully opened conformation (state 3) starting from the lysozyme binding site, the 3D-conformational network is represented just for the unbound state and over the regulatory alfa-helix showing different topology associated and patterns of connectivity across the evaluated conformational states (state 1 to 3). In the left (G-L), are depicted the 3D-structure of the lysozyme-based on the distributions and intensity of allosteric signal propagations and the corresponding 2D-correlation transition matrix (or M_{ij}-based flexibility/rigidity index) of the inter-residue communication network where color intensity bar blue-to-yellow labelled regions correspond to low-to-moderate signal propagation and orange-to-dark red correspond to regions with high propensity to allosteric signal propagation.

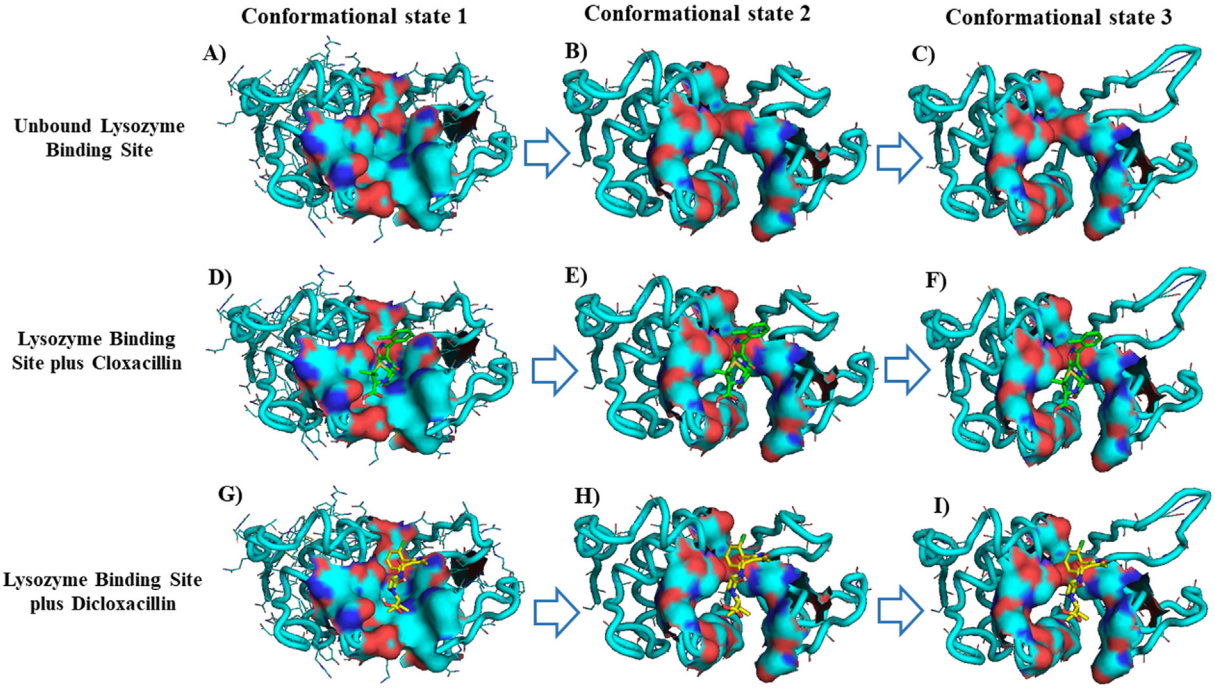

Fig. 8. Schematic 3D-representation of the main lysozyme binding pocket in the best-ranked collective normal modes (or conformational states 1, 2, and 3). Herein, is depicted the three simulation conditions as: A-C) unbound lysozyme, the bound state represented by D-F) cloxacillin/lysozyme docking complex, and G-I) dicloxacillin/lysozyme docking complex considering the conformational state of the main binding site from pseudo-open conformation (state 1) to the fully opened conformation (state 3).

4. Conclusions

In this study we have characterized the physical basis and fundamentals involved in the binding process between lysozyme and two penicillins that differ in a single atom (H and Cl, respectively). The performed 2D-lig-plot diagrams revealed that the most relevant penicillin-lysozyme interactions are essentially based on a predominance of aromatic hydrophobic van der Waals interactions like aromatic π-π stacking. Followed by conventional hydrogen bond interactions which contribute to the stability in the case cloxacillin-lysozyme docking complex. These conclusions were confirmed by microcalorimetry and fluorescence measurements. On the other hand, the best-ranked conformations of the complex obtained by molecular docking confirm the static quenching mechanism suggested by fluorescence experiments, this is, the penicillins and the residues are very close. Besides, performed mechanistic approaches using conformational network models with allosteric signal propagation analysis revealed that both penicillins; theoretically induce long-distance allosteric signal propagation which strongly suggests non-physiological conformational perturbations in large blocks of lysozyme j-effector residues affecting mainly the conformational dynamics of the network of effector residues (Arg45, Asn46, Thr47, Asp48) composing the regulatory alfa-helix in the low-frequency normal modes 1, 2, 3 closely-associated to the lysozyme biochemical function. In this aspect, it is important to emphasize that the slight dissimilarity of the results in the free energy of interaction that we obtained between ITC and molecular docking was related precisely to this allosteric signal propagation. Finally, we show the significant relevance of the balance between the conformational flexibility and rigidity index analysis to capture the intrinsic dynamic function of the lysozyme under theoretical physiological conditions and under the unbound state with cloxacillin and dicloxacillin. This approach is of paramount relevance because could be efficiently used with experimental data to validate the flexibility/rigidity properties, not only for the lysozyme, but also for large macromolecular systems with a low-computational complexity and cost.

CRediT authorship contribution statement

Ramón Rial: Conceptualization, Methodology, Writing – original draft, Writing – review & editing. **Michael González-Durruthy:** Conceptualization, Methodology, Writing – original draft, Writing – review & editing. **Zhen Liu:** . **Juan M. Ruso:** Conceptualization, Methodology, Writing – review & editing.

Declaration of Competing Interest

The authors declare that they have no known competing financial interests or personal relationships that could have appeared to influence the work reported in this paper.

Acknowledgements

The authors acknowledge Ministerio de Ciencia e Innovación (PID2019-111327GB-100)

Appendix A. Supplementary data

Supplementary data to this article can be found online at https://doi.org/10.1016/j.molliq.2022.119081.

References

[1] I.M. Klotz, D.L. Hunston, "Protein interactions with small molecules. Relationships between stoichiometric binding constants, site binding constants, and empirical binding parameters," (in eng), J. Biol. Chem. 250 (8) (1975) 3001–3009.
[2] A. McFedries, A. Schwaid, A. Saghatelian, Methods for the Elucidation of Protein-Small Molecule Interactions, Chem. Biol. 20 (5) (2013) 667–673.
[3] N. Hassan, L.R.S. Barbosa, R. Itri, J.M. Ruso, Fibrinogen stability under surfactant interaction, J. Colloid Interface Sci. 362 (1) (2011) 118–126.
[4] R. Harada, N. Tochio, T. Kigawa, Y. Sugita, M. Feig, Reduced Native State Stability in Crowded Cellular Environment Due to Protein-Protein Interactions, J. Am. Chem. Soc. 135 (9) (2013) 3696–3701.
[5] P. Taboada, V. Mosquera, J.M. Ruso, F. Sarmiento, M.N. Jones, Interaction between Penicillins and Human Serum Albumin: A Thermodynamic Study of Micellar-like Clusters on a Protein, Langmuir 16 (3) (2000.) 934–938.
[6] P. Qin, B. Su, and R. Liu, "Probing the binding of two fluoroquinolones to lysozyme: a combined spectroscopic and docking study," *Molecular BioSystems,* 10.1039/C2MB05423J vol. 8, no. 4, pp. 1222-1229, 2012.
[7] S. Rudra, A. Jana, N. Sepay, B. K. Patel, and A. Mahapatra, "Characterization of the binding of strychnine with bovine β-lactoglobulin and human lysozyme using spectroscopic, kinetic and molecular docking analysis," *New J. Chemistry,* 10.1039/C8NJ00810H vol. 42, no. 11, pp. 8615-8628, 2018.
[8] A. Ghosh, K.V. Brinda, S. Vishveshwara, Dynamics of Lysozyme Structure Network: Probing the Process of Unfolding, Biophys. J . 92 (7) (2007) 2523–2535.
[9] G. Paramaguru, A. Kathiravan, S. Selvaraj, P. Venuvanalingam, R. Renganathan, Interaction of anthraquinone dyes with lysozyme: Evidences from spectroscopic and docking studies, J. Hazard. Mater. 175 (1-3) (2010) 985–991.
[10] Q. Yue, L. Niu, X. Li, X. Shao, X. Xie, Z. Song, "Study on the interaction mechanism of lysozyme and bromophenol blue by fluorescence spectroscopy," (in eng), J Fluoresc 18 (1) (2008) 11–15.
[11] A. Das, R. Thakur, A. Dagar, and A. Chakraborty, "A spectroscopic investigation and molecular docking study on the interaction of hen egg white lysozyme with liposomes of saturated and unsaturated phosphocholines probed by an anticancer drug ellipticine," *Physical Chemistry Chemical Physics,* 10.1039/C3CP54247E vol. 16, no. 11, pp. 5368-5381, 2014.
[12] H. Cai and P. Yao, "In situ preparation of gold nanoparticle-loaded lysozyme–dextran nanogels and applications for cell imaging and drug delivery," *Nanoscale,* 10.1039/C3NR00178D vol. 5, no. 7, pp. 2892-2900, 2013.
[13] M. Haas et al., Drug-targeting to the kidney: Renal delivery and degradation of a naproxen-lysozyme conjugate in vivo, Kidney Int. 52 (6) (1997) 1693–1699.
[14] S. Kalita, R. Kandimalla, A.C. Bhowal, J. Kotoky, S. Kundu, Functionalization of β-lactam antibiotic on lysozyme capped gold nanoclusters retrogress MRSA and its persisters following awakening, Sci. Rep. 8 (1) (2018) 5778.
[15] K. Zheng, M.I. Setyawati, T.-P. Lim, D.T. Leong, J. Xie, Antimicrobial Cluster Bombs: Silver Nanoclusters Packed with Daptomycin, ACS Nano 10 (8) (2016) 7934–7942.
[16] P. Taboada, D. Attwood, J.M. Ruso, M. Garcıa, F. Sarmiento, V. Mosquera, Influence of Molecular Structure on the Ideality of Mixing in Micelles Formed in Binary Mixtures of Surface-Active Drugs, J. Colloid Interface Sci. 216 (2) (1999) 270–275.
[17] P. Taboada, D. Attwood, J.M. Ruso, F. Sarmiento, V. Mosquera, Self-Association of Amphiphilic Penicillins in Aqueous Electrolyte Solution: A Light-Scattering and NMR Study, Langmuir 15 (6) (1999) 2022–2028.
[18] N. Funasaki, S. Hada, S. Neya, Self-Association of Penicillins in Aqueous Solution as Revealed by Gel Filtration Chromatography, Chem. Pharm. Bull. 42 (4) (1994) 779–785.
[19] J.T. DiPiro, N.F. Adkinson Jr., R.G. Hamilton, "Facilitation of penicillin haptenation to serum proteins," (in eng), Antimicrob. Agents Chemother. 37 (7) (1993) 1463–1467.
[20] P. Taboada, V. Mosquera, J.M. Ruso, F. Sarmiento, M.N. Jones, Interaction between Penicillins and Human Serum Albumin: A ζ-Potential Study, Langmuir 16 (17) (2000) 6795–6800.
[21] M. González-Durruthy, R. Rial, M.N.D.S. Cordeiro, Z. Liu, J.M. Ruso, Exploring the conformational binding mechanism of fibrinogen induced by interactions with penicillin β-lactam antibiotic drugs, J. Mol. Liq. 324 (2021.) 114667.
[22] S. Hochreiter, G. Klambauer, M. Rarey, Machine Learning in Drug Discovery, J. Chem. Inf. Model. 58 (9) (2018) 1723–1724.
[23] X.-Y. Meng, H.-X. Zhang, M. Mezei, M. Cui, Molecular Docking: A Powerful Approach for Structure-Based Drug Discovery, Curr. Comput. Aided Drug Des. 7 (2) (2011) 146–157.
[24] M. González-Durruthy, G. Scanavachi, R. Rial, Z. Liu, M.N.D.S. Cordeiro, R. Itri, J. M. Ruso, Structural and energetic evolution of fibrinogen toward to the betablocker interactions, Int. J. Biol. Macromol. 137 (2019) 405–419.
[25] R. Rial, M. González-Durruthy, M. Somoza, Z. Liu, J.M. Ruso, Unraveling the Compositional and Molecular Features Involved in Lysozyme-Benzothiazole Derivative, Interactions 26 (19) (2021) 5855.
[26] T. Wiseman, S. Williston, J.F. Brandts, L.-N. Lin, Rapid measurement of binding constants and heats of binding using a new titration calorimeter, Anal. Biochem. 179 (1) (1989) 131–137.
[27] S. Preus, K. Kilså, F.-A. Miannay, B. Albinsson, and L. M. Wilhelmsson, "FRETmatrix: a general methodology for the simulation and analysis of FRET in nucleic acids," *Nucleic acids research,* vol. 41, no. 1, pp. e18-e18, 2013.
[28] S. Preus, "DecayFit—Fluorescence Decay Analysis Software 1.3, FluorTools," *http://www.fluortools.com,* 2014.
[29] H.M. Berman et al., The protein data bank, Nucleic Acids Res. 28 (1) (2000) 235–242.

[30] O. Trott, A.J. Olson, AutoDock Vina: improving the speed and accuracy of docking with a new scoring function, efficient optimization, and multithreading, J. Comput. Chem. 31 (2) (2010) 455–461.
[31] S. Forli, R. Huey, M.E. Pique, M.F. Sanner, D.S. Goodsell, A.J. Olson, Computational protein–ligand docking and virtual drug screening with the AutoDock suite, Nat. Protoc. 11 (5) (2016) 905–919.
[32] M.D. Hanwell, D.E. Curtis, D.C. Lonie, T. Vandermeersch, E. Zurek, G.R. Hutchison, Avogadro: an advanced semantic chemical editor, visualization, and analysis platform, J. Cheminf. 4 (1) (2012) 1–17.
[33] A. Tao, Y. Huang, Y. Shinohara, M.L. Caylor, S. Pashikanti, D. Xu, ezCADD: A rapid 2D/3D visualization-enabled web modeling environment for democratizing computer-aided drug design, J. Chem. Inf. Model. 59 (1) (2019) 18–24.
[34] J. Jiménez, S. Doerr, G. Martínez-Rosell, A.S. Rose, G. De Fabritiis, DeepSite: protein-binding site predictor using 3D-convolutional neural networks, Bioinformatics 33 (19) (2017) 3036–3042.
[35] W.P. Feinstein, M. Brylinski, Calculating an optimal box size for ligand docking and virtual screening against experimental and predicted binding pockets, J. Cheminf. 7 (1) (2015) 1–10.
[36] R.A. Laskowski, M.B. Swindells, LigPlot+: Multiple Ligand–Protein Interaction Diagrams for Drug Discovery, J. Chem. Inf. Model. 51 (10) (2011) 2778–2786.
[37] B.H. Lee, S. Seo, M.H. Kim, Y. Kim, S. Jo, M.-k. Choi, H. Lee, J.B. Choi, M.K. Kim, L. M. Espinoza-Fonseca, Normal mode-guided transition pathway generation in proteins, PLoS ONE 12 (10) (2017) e0185658, https://doi.org/10.1371/journal.pone.0185658.
[38] F. Tama, F.X. Gadea, O. Marques, Y.-H. Sanejouand, Building-block approach for determining low-frequency normal modes of macromolecules, Proteins: Structure Function, and Bioinformatics 41 (1) (2000) 1–7.
[39] L.-W. Yang, C.-P. Chng, Coarse-Grained Models Reveal Functional Dynamics - I. Elastic Network Models – Theories, Comparisons and Perspectives, Bioinf. Biol. Insights 2 (2008) BBI.S460, https://doi.org/10.4137/BBI.S460.
[40] J.G. Greener, M.J. Sternberg, AlloPred: prediction of allosteric pockets on proteins using normal mode perturbation analysis, BMC Bioinf. 16 (1) (2015) 1–7.
[41] M. Zaman et al., Interaction of anticancer drug pinostrobin with lysozyme: a biophysical and molecular docking approach, J. Biomol. Struct. Dyn. 37 (16) (2019) 4338–4344.
[42] J. Wang *et al.*, "Probing the binding interaction between cadmium(ii) chloride and lysozyme," *New Journal of Chemistry*, 10.1039/C5NJ02911B vol. 40, no. 4, pp. 3738-3746, 2016.
[43] X. Shi, X. Li, M. Gui, H. Zhou, R. Yang, H. Zhang, Y. Jin, Studies on interaction between flavonoids and bovine serum albumin by spectral methods, J. Lumin. 130 (4) (2010) 637–644.
[44] Q. Wang, C.-R. Huang, M. Jiang, Y.-Y. Zhu, J. Wang, J. Chen, J.-H. Shi, Binding interaction of atorvastatin with bovine serum albumin: Spectroscopic methods and molecular docking, Spectrochim. Acta Part A Mol. Biomol. Spectrosc. 156 (2016) 155–163.
[45] Y.-F. Zhang, K.-L. Zhou, Y.-Y. Lou, D.-Q. Pan, J.-H. Shi, Investigation of the binding interaction between estazolam and bovine serum albumin: multi-spectroscopic methods and molecular docking technique, J. Biomol. Struct. Dyn. 35 (16) (2017) 3605–3614.
[46] B.-L. Wang, D.-Q. Pan, K.-L. Zhou, Y.-Y. Lou, J.-H. Shi, Multi-spectroscopic approaches and molecular simulation research of the intermolecular interaction between the angiotensin-converting enzyme inhibitor (ACE inhibitor) benazepril and bovine serum albumin (BSA), Spectrochim. Acta Part A Mol. Biomol. Spectrosc. 212 (2019) 15–24.
[47] J.R. Lakowicz, Principles of fluorescence spectroscopy, Springer science & business media (2013).
[48] M.R. Eftink, Biophysical and Biochemical Aspects of Fluorescence Spectroscopy, Springer US, Boston, MA, 1991, pp. 1–41.
[49] M.S. Ali, H.A. Al-Lohedan, Deciphering the interaction of procaine with bovine serum albumin and elucidation of binding site: A multi spectroscopic and molecular docking study, J. Mol. Liq. 236 (2017) 232–240.
[50] A.M. Jones Brunette, D.L. Farrens, Distance Mapping in Proteins Using Fluorescence Spectroscopy: Tyrosine, like Tryptophan, Quenches Bimane Fluorescence in a Distance-Dependent Manner, Biochemistry 53 (40) (2014) 6290–6301.
[51] S.-B. Kou, Z.-Y. Lin, B.-L. Wang, J.-H. Shi, Y.-X. Liu, Evaluation of the binding behavior of olmutinib (HM61713) with model transport protein: Insights from spectroscopic and molecular docking studies, J. Mol. Struct. 1224 (2021) 129024.
[52] A. Grinvald, I.Z. Steinberg, The fluorescence decay of tryptophan residues in native and denatured proteins, Biochimica et Biophysica Acta (BBA) - Protein Structure 427 (2) (1976) 663–678.
[53] P.D. Ross, S. Subramanian, Thermodynamics of protein association reactions: forces contributing to stability, Biochemistry 20 (11) (1981) 3096–3102.
[54] H. Gohlke and G. Klebe, "Approaches to the Description and Prediction of the Binding Affinity of Small-Molecule Ligands to Macromolecular Receptors," *Angewandte Chemie (International ed. in English)*, vol. 41, pp. 2644-76, 08/02 2002.
[55] P.M. Keen, The binding of penicillins to bovine serum albumin, Biochem. Pharmacol. 15 (4) (1966) 447–463.
[56] R. Huang, B.L.T. Lau, Biomolecule–nanoparticle interactions: Elucidation of the thermodynamics by isothermal titration calorimetry, Biochimica et Biophysica Acta (BBA) - General Subjects 1860 (5) (2016) 945–956.
[57] K.E. Riley et al., Halogen bond tunability I: the effects of aromatic fluorine substitution on the strengths of halogen-bonding interactions involving chlorine, bromine, and iodine, J. Mol. Model. 17 (12) (2011) 3309–3318.
[58] K.E. Riley, P. Hobza, Strength and Character of Halogen Bonds in Protein-Ligand Complexes, Cryst. Growth Des. 11 (10) (2011) 4272–4278.
[59] A. Memic, M.R. Spaller, How Do Halogen Substituents Contribute to Protein-Binding Interactions? A Thermodynamic Study of Peptide Ligands with Diverse Aryl Halides, ChemBioChem 9 (17) (2008) 2793–2795.
[60] E.W. Bell, Y. Zhang, DockRMSD: an open-source tool for atom mapping and RMSD calculation of symmetric molecules through graph isomorphism, J. Cheminf. 11 (1) (2019) 1–9.
[61] T. Oliwa, Y. Shen, cNMA: a framework of encounter complex-based normal mode analysis to model conformational changes in protein interactions, Bioinformatics 31 (12) (2015) i151–i160.
[62] K. Xia, K. Opron, G.-W. Wei, Multiscale multiphysics and multidomain models—Flexibility and rigidity, J. Chem. Phys. 139 (19) (2013) 194109, https://doi.org/10.1063/1.4830404.
[63] Z. Chen et al., D3Pockets: a method and web server for systematic analysis of protein pocket dynamics, J. Chem. Inf. Model. 59 (8) (2019) 3353–3358.
[64] C. Chennubhotla, I. Bahar, M. Levitt, Signal propagation in proteins and relation to equilibrium fluctuations, PLoS Comput. Biol. 3 (9) (2007) e172, https://doi.org/10.1371/journal.pcbi.0030172.